Novel cell death program leads to neutrophil extracellular traps

Tobias A. Fuchs,[1,5] Ulrike Abed,[1,2] Christian Goosmann,[1,2] Robert Hurwitz,[3] Ilka Schulze,[4] Volker Wahn,[4] Yvette Weinrauch,[5] Volker Brinkmann,[2] and Arturo Zychlinsky[1]

[1]Department for Cellular Microbiology, [2]Microscopy Core Facility, and [3]Protein Purification Core Facility, Max-Planck Institute for Infection Biology, 10117 Berlin, Germany
[4]Department for Paediatric Pneumology and Immunology, Charité Universitätsmedizin Berlin, 13353 Berlin, Germany
[5]Department of Microbiology, New York University School of Medicine, New York, NY 10016

Neutrophil extracellular traps (NETs) are extracellular structures composed of chromatin and granule proteins that bind and kill microorganisms. We show that upon stimulation, the nuclei of neutrophils lose their shape, and the eu- and heterochromatin homogenize. Later, the nuclear envelope and the granule membranes disintegrate, allowing the mixing of NET components. Finally, the NETs are released as the cell membrane breaks. This cell death process is distinct from apoptosis and necrosis and depends on the generation of reactive oxygen species (ROS) by NADPH oxidase. Patients with chronic granulomatous disease carry mutations in NADPH oxidase and cannot activate this cell-death pathway or make NETs. This novel ROS-dependent death allows neutrophils to fulfill their antimicrobial function, even beyond their lifespan.

Introduction

Neutrophils are one of the first lines of defense against invading microbes (Kanthack and Hardy, 1895; Nathan, 2006). These cells are terminally differentiated, and they have a short life span and low levels of gene expression. When they reach the circulation, they are already equipped with the proteins required to kill microorganisms (Borregaard and Cowland, 1997). Neutrophils in circulation are directed by cytokines into infected tissues, where they encounter invading microbes. This encounter leads to the activation of neutrophils and the engulfment of the pathogen into a phagosome. In the phagosome, two events are required for antimicrobial activity. First, the presynthesized subunits of the NADPH oxidase assemble at the phagosomal membrane and transfer electrons to oxygen to form superoxide anions. These dismutate spontaneously or catalytically to dioxygen and hydrogen peroxide. Collectively, superoxide anions, dioxygen, and hydrogen peroxide are called reactive oxygen species (ROS; Hampton et al., 1998). Second, the granules fuse with the phagosome, discharging antimicrobial peptides and enzymes. In the phagosome, microorganisms are exposed to high concentrations of ROS and antimicrobial peptides. Together, they are responsible for microbial killing (Klebanoff, 1999). Patients with mutations in the NADPH oxidase suffer from chronic granulomatous disease (CGD; Heyworth et al., 2003). CGD patients are severely immunodeficient, have recurrent infections, often with opportunistic pathogens, and have poor prognosis.

Recently, we described a novel antimicrobial mechanism of neutrophils. Upon activation, neutrophils release extracellular traps (neutrophil extracellular traps [NETs]; Brinkmann et al., 2004). NETs are composed of chromatin decorated with granular proteins. These structures bind Gram-positive and -negative bacteria, as well as fungi (Urban et al., 2006). NETs provide a high local concentration of antimicrobial molecules that kill microbes effectively. NETs are abundant at inflammatory sites, as shown for human appendicitis and an experimental model of shigellosis. Recently, NETs were shown to be relevant in vivo in human preeclampsia (Gupta et al., 2005) and streptococcal infections (Molloy, 2006), causing necrotizing fasciitis (Buchanan et al., 2006) and pneumococcal pneumonia (Beiter et al., 2006).

The release of intact chromatin decorated with cytoplasmic proteins into the extracellular space is unprecedented. We describe that activated neutrophils initiate a process where first the classical lobulated nuclear morphology and the distinction between eu- and heterochromatin are lost. Later, all the internal membranes disappear, allowing NET components to mix. Finally, NETs emerge from the cell as the cytoplasmic membrane is

V. Brinkmann and A. Zychlinsky contributed equally to this paper.

Correspondence to Arturo Zychlinsky: zychlinsky@mpiib-berlin.mpg.de

Abbreviations used in this paper: AT, 3-amino-1,2,4-triazole; CGD, chronic granulomatous disease; DPI, diphenylene iodonium; GO, glucose oxidase; IL, interleukin; LPS, lipopolysaccharide; MNase, micrococcal nuclease; MOI, multiplicity of infection; NETs, neutrophil extracellular traps; PBMC, peripheral blood mononuclear cells; PS, phosphatidylserine; ROS, reactive oxygen species.

The online version of this article contains supplemental material.

The Journal of Cell Biology, Vol. 176, No. 2, January 15, 2007 231–241
http://www.jcb.org/cgi/doi/10.1083/jcb.200606027

ruptured by a process that is distinct from necrosis or apoptosis. This active process is dependent on the generation of ROS by NADPH oxidase. In an infection, ROS formation may contribute to the following two antimicrobial pathways: intraphagosomal killing in live neutrophils and NET-mediated killing post mortem.

Results

NETs are formed during active cell death

To analyze NET formation, we monitored individual neutrophils with live-cell imaging through four different channels. First, we recorded the phase-contrast image to determine the morphology. Second, to assess cell viability, neutrophils were loaded with calcein blue, a dye that is retained in the cytoplasm of living cells and rapidly lost upon cell death. Third, the neutrophils were incubated in the presence of Annexin V, which binds to phosphatidylserine (PS). PS is localized to the inner leaflet of the cell membrane. Annexin V can only bind to PS of cells undergoing apoptosis, when PS is transferred to the outer leaflet, or after membrane rupture, when Annexin V can enter into the cell. Thus, if the plasma membrane breaks, the cells lose the vital dye and are stained with Annexin V simultaneously. If a cell undergoes apoptosis, it will first become Annexin V–positive and later lose the vital dye. Fourth, to detect the appearance of NETs, we used fluorescently labeled Fab fragments of monoclonal antibodies against the complex composed of histone 2A, histone 2B, and DNA (Fig. 1 and Video 1, available at http://www.jcb.org/cgi/content/full/jcb.200606027/DC1; Losman et al., 1992) or neutrophil elastase (Fig. S3 and Video 2). In viable neutrophils, neither Fabs nor Annexin V have access to their targets. When NETs emerge or cells die, Fabs and Annexin V can bind; because of the increase in the local concentration, they become detectable.

Purified peripheral blood neutrophils were activated with PMA and monitored by live-cell imaging for 240 min. Initially, neutrophils flattened and formed numerous intracellular vacuoles (Fig. 1 a and Video 1). After 80 min, nuclei lost their lobular shape, and they expanded and filled most of the intracellular space (Fig. 1 b). At this time, the cells were viable because they retained calcein blue (Fig. 1, b and h, blue) and excluded Annexin V (green). After 220 min of activation, progressively more cells lost the calcein blue marker and concurrently stained with Annexin V (Fig. 1, d, j, and p), indicating rupture of the plasma membrane.

NETs only became detectable when the cell membrane was ruptured. As shown in Fig. 1, NETs (Fig. 1 p, red) appeared exactly when cells lost the vital dye and simultaneously became positive for Annexin V (Fig. 1 j). This clearly demonstrates that NETs emerge from dying neutrophils. This also shows that NETs are not released by apoptotic neutrophils because PS was not exposed before the rupture of the plasma membrane, which is indicated by the loss of calcein blue. In contrast, apoptotic

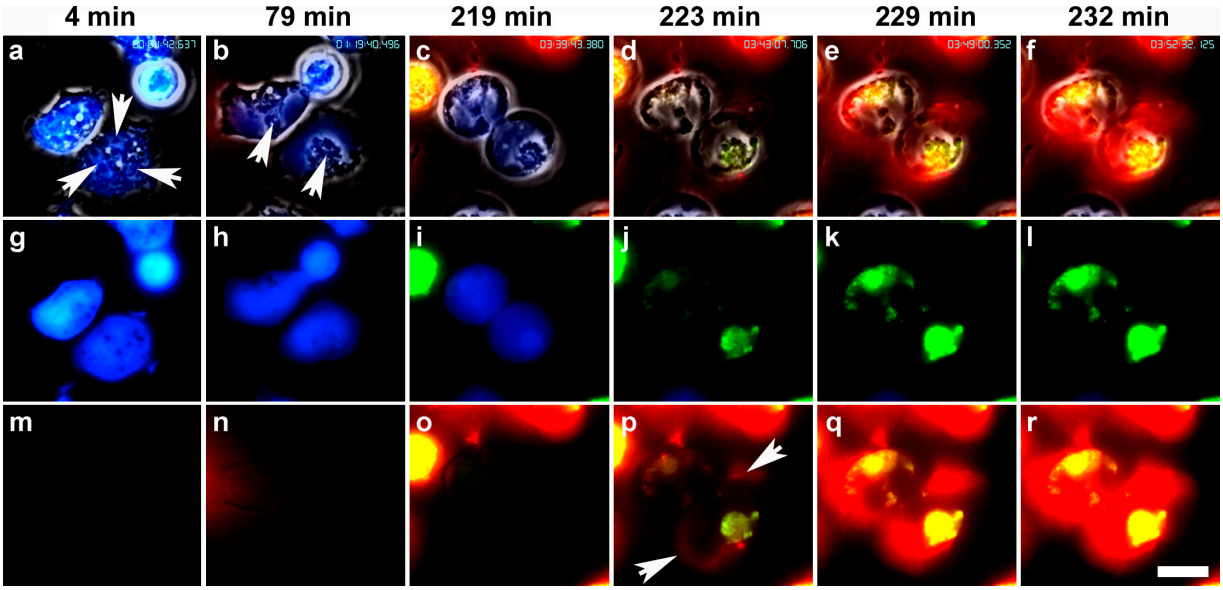

Figure 1. **Neutrophils die an active form of cell death to release NETs.** Neutrophils were activated with 20 nM PMA and monitored by live-cell imaging (Video 1) in four different channels: phase contrast, with the vital dye calcein blue, with the cell death marker Annexin V (green), and with Fabs against a histone–DNA complex (red). (a–f) Merge of all four channels. (g–l) Merge of calcein blue and Annexin V channels. (m–r) Merge of Annexin V and anti–histone–DNA Fabs. The cells were monitored for up to 4 h, and key indicated time points are shown. (a) Shortly after stimulation, neutrophils show a multitude of granules and a lobulated nucleus (arrows). All cells are viable, as indicated by the vital dye calcein blue AM staining. (b) After 79 min of stimulation, the cells are flat; their nuclei are no longer lobulated and occupy the entire cell, except for a small area with residual granules (arrows). (c and i) After 219 min, the two cells in the center start to round up and are still viable. (d, j, and p) 4 min later the plasma membranes rupture, indicated by the simultaneous loss of calcein blue staining and the positive signal for Annexin V. (p) A light red staining in the periphery of the cell indicates NET formation (arrows). (e, q, f, and r) In the next few minutes, the signal of a Fab against the histone–DNA complex gets brighter and remains throughout the duration of the experiment, indicating that NET components do not diffuse after membrane rupture, but form a stable structure. At 219 min, a necrotic cell (loss of calcein blue AM, intracellular staining with Annexin V, and intracellular staining with histone–DNA complex) floated into the microscopic field. The figure shows a detail of a larger field of view that contained 20 cells, 10 of which formed NETs between 70 and 240 min after stimulation. Video 1 is available at http://www.jcb.org/cgi/content/full/jcb.200606027/DC1. Bar, 10 μm.

neutrophils became Annexin V positive before the integrity of the plasma membrane was compromised (unpublished data). Controls with Fabs against irrelevant antigens did not stain the NETs (unpublished data). The process of NET formation was identical when neutrophils were seeded on plastic, glass, or collagen-coated glass.

Morphological analysis of neutrophil activation leading to cell death

To investigate the morphological changes leading to the cell death and NET formation, we fixed neutrophils at different time points after activation and analyzed their morphology by transmission electron and fluorescence microscopy. 60 min after stimulation, the nuclei started to lose their lobules, and the chromatin began to decondense while the nuclear membrane remained intact (Fig. 2, b and f). At this time point, the space between the inner and outer nuclear membrane dilated (0 min, 18.8 ± 3.9 nm; 60 min, 27.9 ± 5.8 nm). 120 min after stimulation, the nuclear membranes formed distinct vesicles (Fig. 2, c and g), and by 180 min the nuclear envelope disintegrated into numerous small vesicles and the chromatin decondensed (Fig. 2, d and h). These vesicles originated from the nuclear envelope, as demonstrated by immune detection of the lamin B receptor, which is a component of the inner nuclear membrane

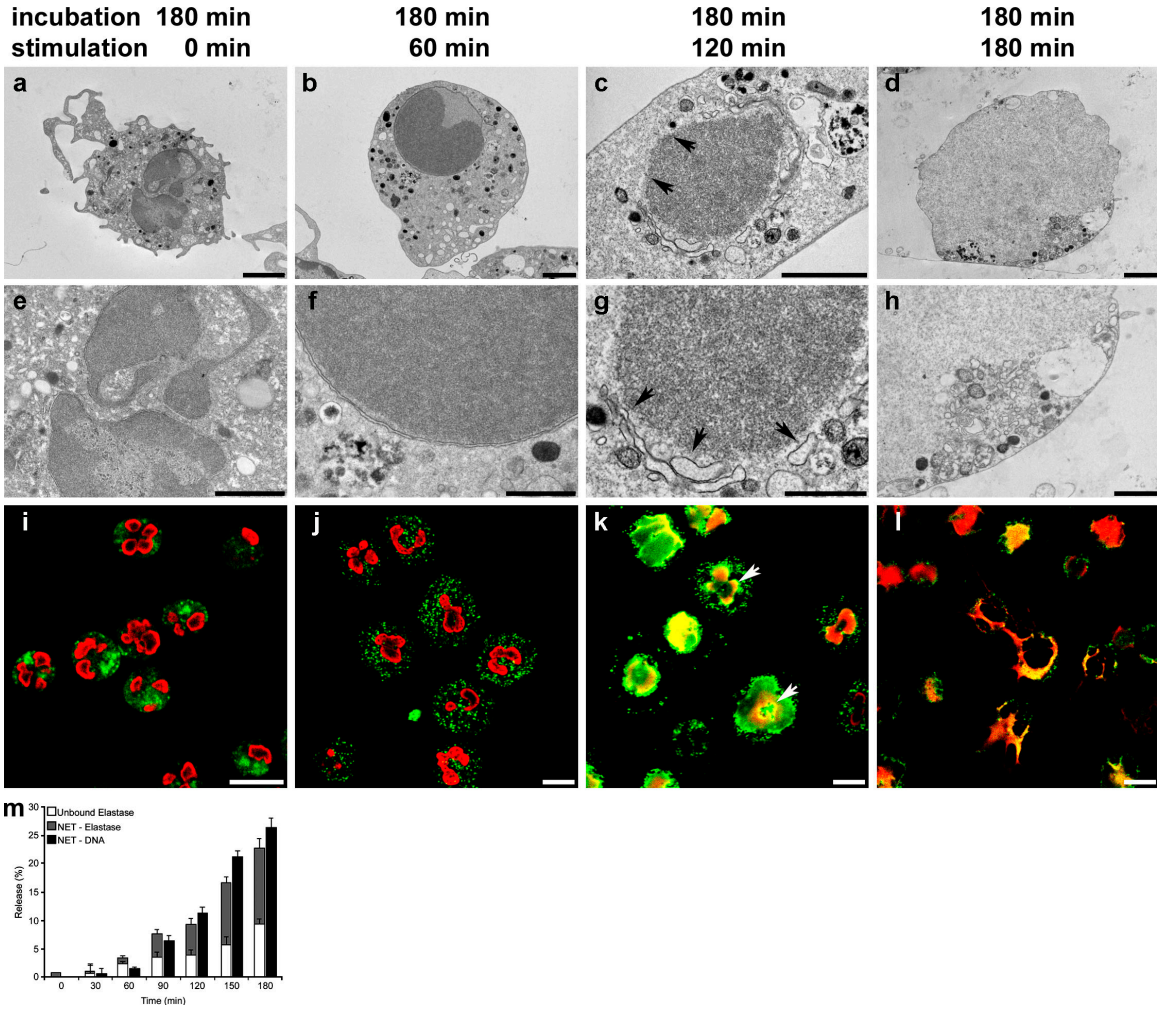

Figure 2. **Disintegration of the nucleus and granules allows the formation of NETs.** Transmission electron microscopy (a–h) and confocal immunomicroscopy (i–l) of neutrophils. Cells were incubated for 180 min in medium without stimulation (a, e, and i) or activated with 20 nM PMA for 60 (b, f, and j), 120 (c, g, and k), or 180 min (d, h, and l; all incubated for a total of 180 min). e–h are higher magnifications of a–d. (a and e) Naive neutrophils show a lobulated nucleus with clearly defined eu- and heterochromatin and numerous cytoplasmic vacuoles, even after 180 min of incubation. (i) Immunofluorescence staining for nuclear (red, histone–DNA complex antibodies) and granular components (green, neutrophil elastase antibodies) is clearly separated in naive neutrophils. Granules are distributed through the globular cell and exhibit a patchy cytoplasmic pattern in this projection of a confocal z stack. (b) After 60 min of stimulation, nuclei are less lobulated. (f) The space between inner and outer nuclear membrane is dilated. (j) Nuclei and granules are now individually visible because the cell has flattened out. (c) After 120 min, most nuclei no longer show separation of eu- and heterochromatin, and in some cells the nuclear envelope starts to disintegrate into a chain of vesicles surrounding the DNA (arrows). (g) DNA and cytoplasm are no longer separated by a membrane (arrows). (k) Cells lose their distinct granule pattern and show colocalization (yellow) of neutrophil elastase (green) and chromatin (red), especially at the nuclear periphery (arrows). (d) Most neutrophils stimulated for 180 min are nearly entirely filled with decondensed chromatin. (h) Small areas are occupied with residual granules and numerous vesicles. (l) Some cells already released NETs. (m) Extracellular neutrophil elastase was measured as described in Materials and methods. By 180 min, most of the neutrophil elastase was bound to chromatin (gray). The timecourse of release correlates with NET-DNA release (black). The experiment was repeated at least three times with neutrophils from independent donors, with similar results. The data shown is a representative triplicate experiment and presented as a mean value ± the SD. Bars: (a–d) 2 μm; (e–h) 1 μm; (i–l) 10 μm.

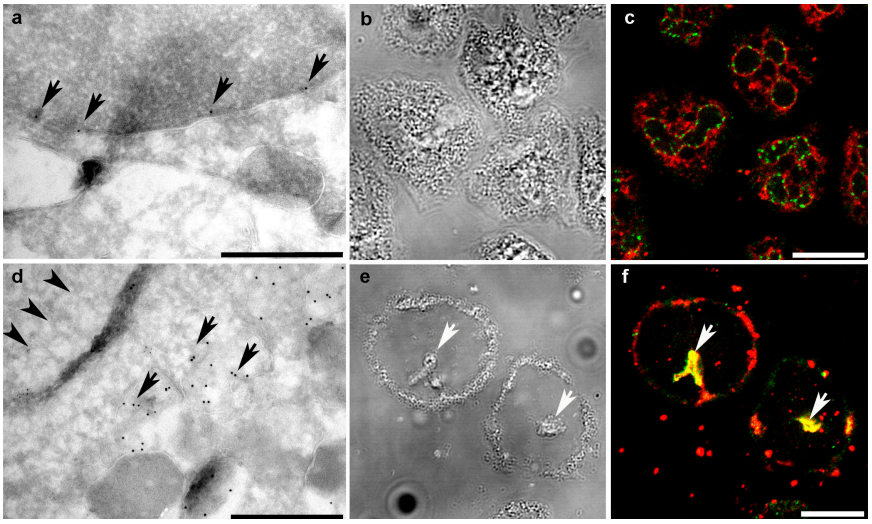

Figure 3. **The nuclear membrane vesiculates after activation.** Ultrathin cryosections of neutrophils stimulated with 20 nM PMA for 60 (a) and 180 (d) min and labeled with an antibody against the nuclear envelope–specific lamin B receptor. Bound antibody was detected with a gold-conjugated secondary antibody. In 60-min–stimulated neutrophils, the lamin B receptor was found on the inner nuclear membrane, as expected (a, arrows). 180 min after stimulation, the lamin B receptor was found in vesicles (d, arrows) in the cytoplasm. Nuclear material (d, arrowheads) is decondensed and not enclosed by a membrane. (b) 60 min after activation, neutrophils have flattened out and exhibit a lobulated nucleus and numerous granules. (c) Immunofluorescence staining for the nuclear membrane delineates the nuclear lobules (green) and is in continuity with the endoplasmic reticulum (red). (e and f) After 180 min of stimulation, neutrophil nuclei are inflated and fill nearly the entire cell. Some remaining granules are found in the periphery of the cell, while remnants of the nuclear membrane and the endoplasmic reticulum are restricted to a small central area surrounded by nuclear material (arrows). Bars: (a and d) 500 nm; (b, c, e, and d) 10 μm.

(Fig. 3, a and d; Worman et al., 1988), and by immunofluorescence staining of nuclear membrane proteins (Fig. 3, c and f). By 180 min, most granules disappeared (Fig. 2, d and h).

With the loss of nuclear and granular membranes, the decondensed chromatin came into direct contact with cytoplasmic and granular components. We showed by immunofluorescence that 120 min after activation the granular marker neutrophil elastase colocalized with chromatin, although some granular punctuate staining remained (Fig. 2 k). Later in the activation, the granular staining was lost and all the neutrophil elastase was associated with chromatin (Fig. 2 l). The intracellular mixing of granular components and chromatin was supported by the observation that most of the neutrophil elastase released by the cell remained bound to NETs (Fig. 2 m). Interestingly, the plasma membrane integrity of activated neutrophils was not affected by disruption of internal membranes, allowing the intracellular mixing of NET components (Fig. 2 d). Similar morphological changes were observed when neutrophils were infected with bacteria (Fig. 5).

NET-forming death is different from necrosis and apoptosis

We compared the cell death that leads to NET formation to apoptosis and necrosis. We induced apoptosis (Fig. 4 a) by incubating neutrophils with anti-Fas antibodies for 18 h (Fadeel et al., 1998). In these conditions, ~70% of the cells were dead. Apoptotic neutrophils showed the classical morphology, including condensation of chromatin and fragmentation of nuclei

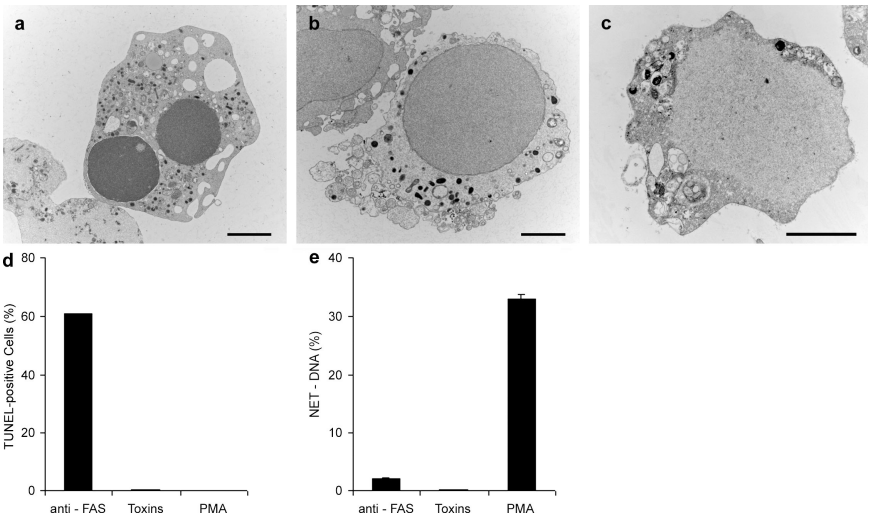

Figure 4. **Neither apoptosis nor necrosis induce NETs.** Neutrophils were stimulated with 20 ng/ml anti-Fas antibodies for 18 h to induce apoptosis, incubated with 25 μg/ml of pore-forming secreted toxins from *S. aureus* for 15 min to induce necrosis, or activated with 10 nM PMA for 4 h to induce NETs. (a–c) Transmission electron micrographs. (a) Neutrophil treated with anti-Fas antibodies show characteristic apoptotic morphology, including nuclear condensation and fragmentation as well as cytoplasmic vacuolization. (b) Features of necrosis in neutrophils treated with toxins are the loss of segregation into eu- and heterochromatin and of the nuclear lobules. The nuclear envelope, as well as the granules, remains intact. (c) Neutrophils undergoing NET-forming active cell death exhibit a morphology clearly different from both apoptosis and necrosis. The nuclear membranes are entirely fragmented while most of the granules are dissolved, allowing direct contact and mixing of nuclear, cytoplasmic, and granular components. Bars, 2 μm. (d) TUNEL analysis of different forms of cell death reveals that 60% of the anti-Fas–treated neutrophils have fragmented DNA, whereas toxin- and PMA-treated neutrophils do not. $n = 200$ cells/condition. (e) Neither apoptosis nor necrosis lead to NET formation, as revealed by quantifying extracellular DNA. The experiment was repeated at least three times with neutrophils from independent donors with similar results. The data shown is a representative triplicate experiment and presented as a mean value ± the SD.

without rupture of the nuclear envelope, as well as cytoplasmic vacuolization. Organelles in the cytoplasm remained intact. Neutrophils incubated with high concentrations of secreted pore-forming toxins from *Staphylococcus aureus* for 15 min when >70% of the cells were dead showed typical necrotic morphology (Fig. 4 b; Genestier et al., 2005). The nuclei lost their structure, and lobules fused into a homogenous mass without segregation into eu- and heterochromatin and did not make NETs, even in long incubation periods. In contrast to cells forming NETs (Fig. 4 c), the nuclear membranes remained intact and clearly separated nucleoplasm from cytoplasm. The structure of organelles was not affected. Fig. 4 c shows a neutrophil activated with PMA for 4 h to promote NET formation. The most salient morphological differences in comparison to the apoptotic and necrotic cells are disintegration of the nuclear envelope and mixing of nuclear and cytoplasmic material, loss of internal membranes, and disappearance of cytoplasmic organelles. Neutrophils activated with PMA did not proceed to have a necrotic morphology, even after longer incubation.

DNA fragmentation, as detected by TUNEL, is a hallmark of apoptosis and was only apparent after stimulation with anti-Fas antibodies (Fig. 4 d), but not when the cells died by necrosis after incubation with *S. aureus* toxins. Neutrophils activated to make NETs were also TUNEL negative. We quantified NET formation under these different conditions by digesting the DNA scaffold of NETs with an endonuclease and measuring the

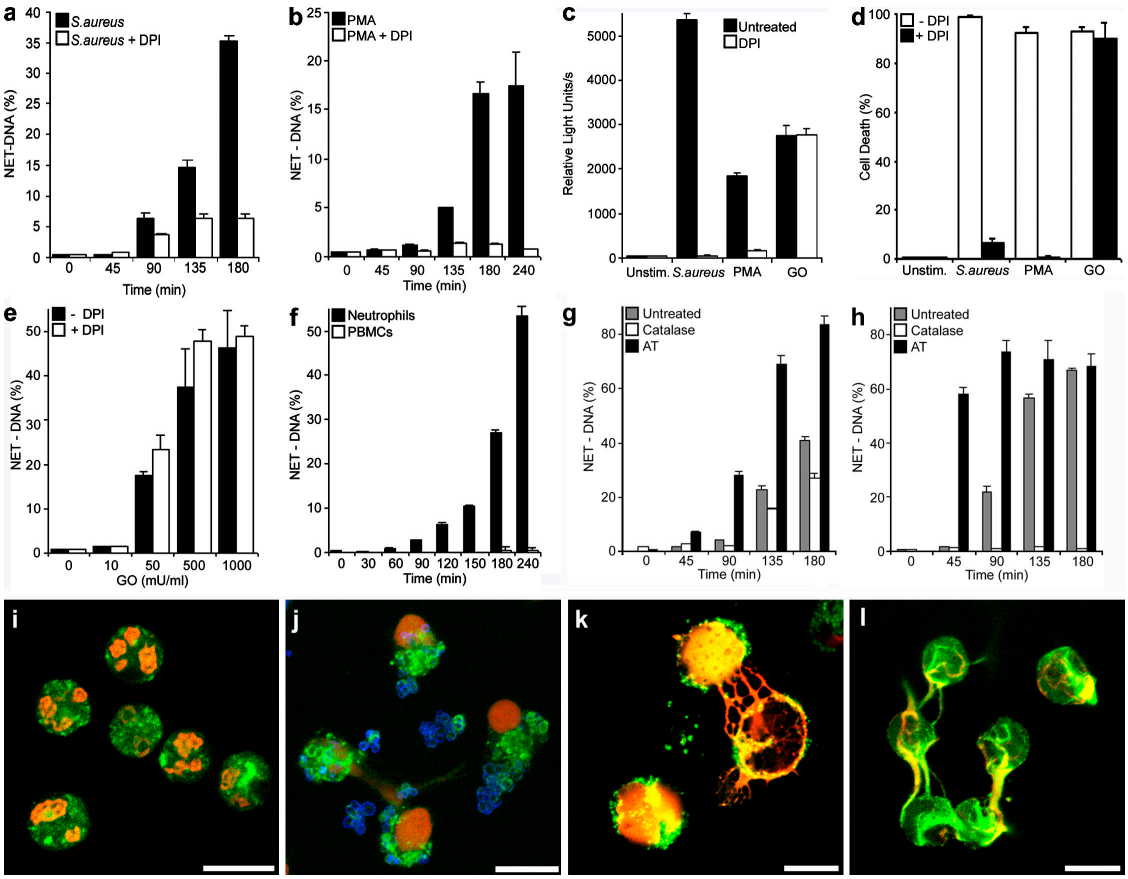

Figure 5. **NET-forming cell death depends on ROS production.** (a) NET-DNA quantification of neutrophils stimulated with *S. aureus* (multiplicity of infection [MOI] 20) in the absence or presence of 10 μM of the NADPH oxidase inhibitor DPI, as indicated in the figure. (b) Quantification of NET formation of PMA-stimulated (10 nM) neutrophils in the absence (closed bars) or presence (open bars) of DPI. (c) ROS production 20 min after activation with *S. aureus* or PMA or 10 min after stimulation with 100 mU/ml GO was comparable (closed bars). After pharmacological inhibition of NADPH oxidase with DPI (open bars), ROS production was blocked when stimulated with *S. aureus* or PMA, but not with GO-treated cells. (d) Neutrophil cell death is dependent on ROS production. Neutrophils were stimulated with *S. aureus* for 180 min and PMA or GO for 240 min, and cell death was determined by vital dye exclusion. Cell death was abrogated by DPI in *S. aureus*– and PMA-, but not GO-, stimulated neutrophils. (e) Neutrophils incubated for 180 min with the indicated concentrations of GO in the absence (closed bars) or presence (open bars) of DPI. NET formation was induced by GO in a dose-dependent manner and was not dependent on NADPH oxidase activity. (f) GO treatment did induce NET formation in neutrophils, but not PBMCs. Neutrophils (closed bars) and PBMCs (open bars) were stimulated with GO for indicated periods and NET formation was quantified. NET-DNA release became detectable 90 min after activation only from neutrophils. (g) Neutrophils were activated with PMA in the presence of exogenous catalases (open bars), an inhibitor of endogenous catalases (AT, closed bars) or in the absence of these components (gray bars). (h) Stimulation of neutrophils with GO in the presence of exogenous catalases (open bars, 100 mU/ml), an inhibitor of endogenous catalases (AT, closed bars, 1 mM) or in the absence of these components (gray bars). In response to both stimuli, PMA and GO exogenous catalases reduced NET formation whereas NET formation was enhanced after inhibition of endogenous catalases as quantified by isolating NET – DNA. (i–l) Immunostaining of NET components (green, neutrophil elastase; red, histone–DNA complex). Bars, 10 μm. (i) Unstimulated neutrophils incubated for 180 min do not show NETs. Neutrophils stimulated with *S. aureus* (j, blue) for 120 min or PMA (k) for 180 min showed NETs. (l) Stimulation with GO for 180 min induced NET formation. The experiment was repeated at least 5 times with neutrophils from independent donors with similar results. The data shown is a representative triplicate experiment and presented as a mean value ± the SD.

content of released DNA in the supernatant (Fig. S1, available at http://www.jcb.org/cgi/content/full/jcb.200606027/DC1). NETs were detected after PMA activation (Fig. 4 e), but not after incubation with Fas antibody or treatment with *S. aureus* toxins. Together, these data indicate that neither apoptosis nor necrosis lead to NET formation, and that NET-inducing cell death is different from both apoptosis and necrosis by morphological and molecular criteria.

NET death is dependent on ROS production

Stimulation of neutrophils with interleukin (IL)-8, lipopolysaccharide (LPS), or PMA (Brinkmann et al., 2004; Gupta et al., 2005) induced NETs as early as 45 min after activation. IL-8– or LPS-activated neutrophils formed NETs above background (Fig. S1 a). The number of NETs were detected microscopically, but were under the detection level of the nuclease method described in Fig. S1 (b–f). We also observed that infection of neutrophils with bacteria produced a robust amount of NETs (Figs. 5 and S1 a) that increased with time. To investigate the mechanism of NET formation, we stimulated neutrophils with the potent activator PMA, as well as with viable bacteria, as a biologically relevant stimulus. As expected, we observed differences in NET formation between different donors (Fig. S5), and experiments are representative and done in triplicate or quadruplicate with neutrophils from a single donor.

Neutrophils infected with *S. aureus* (Fig. 5, a, d, and j) or PMA (Fig. 5, b, d, and k) formed NETs. Typical morphological features, like decondensed nuclei merging with granular components in the cytoplasm, as well as extracellular fibers consisting of DNA, histones, and elastase, were detected after stimulation with both stimuli (Fig. 5, j and k), but not in unstimulated cells (Fig. 5 i). Quantitation of NETs showed that *S. aureus* (Fig. 1 a and Fig. 5 a) induced more NETs, and after 45 min the kinetics are even faster than after stimulation with PMA (Fig. 5 b). It is important to note that in these infections *S. aureus* was grown in conditions where the toxins are not expressed (see Materials and methods).

In these experiments, all cells were incubated for the same amount of time, but stimulated for the indicated periods. That is, cells that were not stimulated (time 0 min) were in fact incubated for the duration of the experiment. Accordingly, cells stimulated for the entire duration of the experiment are shown as 180 (Fig. 5, a, g, and h) or 240 min (Fig. 5, b and f).

Stimulation with live bacteria or PMA triggers the assembly and activation of NADPH oxidase and the production of ROS (Fig. 5 c). Therefore, we tested if this enzyme was required to make NETs. The NADPH oxidase inhibitor diphenylene iodonium (DPI) prevented NET formation (Fig. 5, a and b), ROS production (Fig. 5 c), and cell death (Fig. 5 d) upon activation with *S. aureus* or PMA.

To test whether stimulation of neutrophils downstream of NADPH oxidase produces NETs, we generated hydrogen peroxide exogenously using glucose oxidase (GO) and showed that stimulation with hydrogen peroxide, which is membrane permeable, induces NETs (Fig. 5, e and l). At the concentrations used, GO produced ROS comparable to *S. aureus*– or PMA-stimulated neutrophils (Fig. 5 c). As expected, because hydrogen peroxide stimulates downstream of NADPH oxidase, neutrophils incubated with GO died (Fig. 5 d) and made NETs (Fig. 5 e) even when NADPH oxidase was inhibited. Control experiments demonstrate that NET formation was specific to neutrophils, as stimulation of peripheral blood mononuclear cells (PBMCs) with PMA (unpublished data) or GO did not release any DNA (Fig. 5 f).

To determine whether ROS were regulating the process of NET formation we tested the role of catalase in this process. Catalase converts hydrogen peroxide into water and dioxygen. Accordingly, the presence of exogenous catalases reduced NET formation in response to PMA activation (Fig. 5 g). Catalases completely inhibited NET formation after GO activation, confirming that stimulation by GO is exclusively caused by the production of hydrogen peroxide (Fig. 5 h). Conversely, the inhibition of endogenous catalases with 3-amino-1,2,4-triazole (AT), dramatically increased NETs in response to different stimuli (Fig. 5, g and h). Interestingly, serum has antioxidant activity (Yu, 1994), and, consistently, NET formation is inhibited in a concentration-dependent fashion by serum (Fig. S2, available at http://www.jcb.org/cgi/content/full/jcb.200606027/DC1). Therefore NET induction is optimal at low serum concentrations ($\leq$2%).

ROS requirement for NET formation in CGD patients

Mutations in the phagocyte NADPH oxidase cause CGD. We tested neutrophils isolated from five patients that have mutations in the NADPH oxidase. We confirmed that neutrophils from each of these patients are unable to generate ROS upon PMA activation (Fig. 6 i). The morphology of naive neutrophils isolated from CGD patients is indistinguishable from that of neutrophils isolated from healthy donors (Fig. 6 a). Interestingly, neutrophils isolated from CGD patients activated with *S. aureus* (Fig. 6 b) or PMA (Fig. 6, c, e, and f) did not show NETs and lacked the morphological changes characteristic of NET formation, such as breakdown of the nuclear envelope and the mixing of NET components within the cytoplasm. However, neutrophils from these patients, when stimulated with GO, formed NETs that were similar to those made by neutrophils from healthy donors (Fig. 6, d, g, and h; and Fig. S4 and Video 3, available at http://www.jcb.org/cgi/content/full/jcb.200606027/DC1). Quantification of DNA revealed that CGD neutrophils do not make NETs upon *S. aureus* and PMA activation, but release NETs at normal levels after GO stimulation (Fig. 6 j). Together, the data with ROS inhibitors and from neutrophils isolated from CGD patients show that NADPH oxidase is required to trigger a signal that culminates in the formation of NETs.

Neutrophils kill bacteria efficiently post mortem

We compared the antimicrobial activity of viable, naive neutrophils and neutrophils that formed NETs. Although microbes induce NETs by themselves, in this experiment we synchronized NET formation by preactivating the cells with either

PMA (Fig. 7 a) or GO (Fig. 7 b). After isolation, the stimulus was added to the neutrophils so that by 240 min after the initiation of the experiment, the cells would be stimulated for 0, 60, 120, 180, and 240 min. Next, the stimulus was removed and the cells were incubated in the presence or absence of DNase before infection with *S. aureus*. In the absence of DNase (Fig. 7, untreated), neutrophils can kill the bacteria by both phagocytosis and through NETs. In contrast, in the presence of DNase the NETs are dismantled (Fig. S1 c) and bacterial killing is only mediated by phagocytosis. The differences in bacterial killing in cultures with and without DNase reflect the antimicrobial activity of NETs.

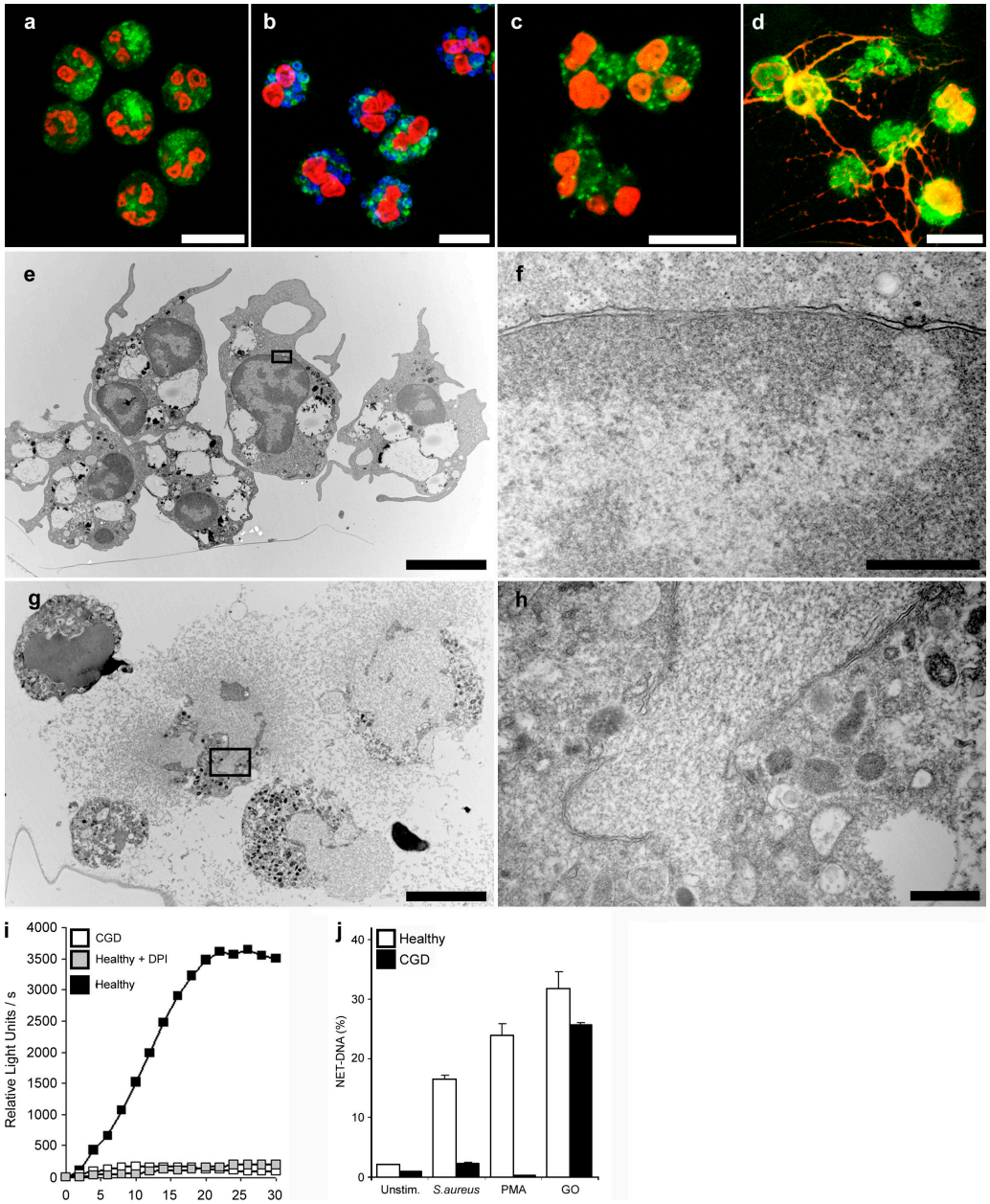

Figure 6. **NADPH oxidase is required to make NETs.** (a–d) Immunostaining for NET components (green, neutrophil elastase; red, histone–DNA complex) of neutrophils isolated from a CGD patient. (a) Unstimulated neutrophils showed a typical lobulated nucleus and a distinct pattern of cytoplasmic granules. After *S. aureus* (b, blue; MOI 20) and 10 nM PMA (c) stimulation, we observed no substantial morphological changes. (d) Stimulation with 100 mU/ml GO elicited NET formation in neutrophils from CGD donors. (e–h) Transmission electron micrographs. Neutrophils isolated from CGD patients 3 h after PMA activation (e and f) showed no morphological signs of NET formation. The nuclei are still lobulated and granules are clearly visible. (g and h) GO-stimulated neutrophils isolated from CGD patients at the moment of NET formation. The plasma membrane ruptured, allowing the release of NETs. The nuclear membrane disintegrated, allowing the mixing of nuclear and granular components. (i) ROS production of PMA-activated neutrophils obtained from healthy donors in the absence or presence of 10 μM DPI and of PMA-activated neutrophils from CGD donors. ROS production was completely blocked by DPI to basal levels, as with neutrophils from CGD donors. (j) Quantification of NET-DNA of normal neutrophils and neutrophils from CGD patients. CGD neutrophils did not make NETs after *S. aureus* or PMA activation, but stimulation with GO elicited NETs to normal levels. The experiment was repeated at least five times with neutrophils from independent donors, with similar results. The data shown is a representative triplicate experiment and presented as a mean value ± the SD. Bars: (a–e and g) 10 μm; (f and h) 1 μm.

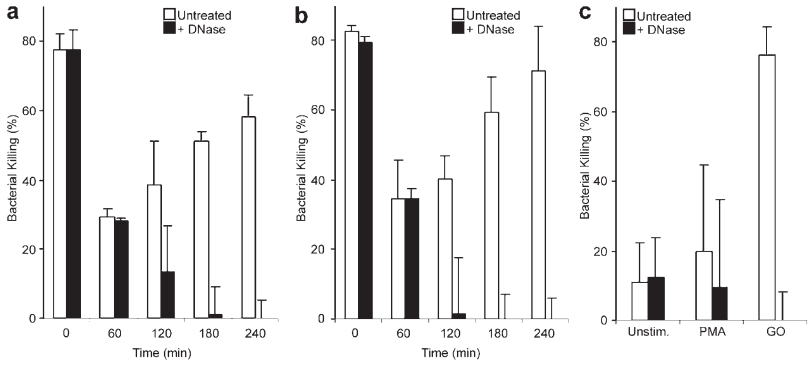

Figure 7. **Neutrophils kill *S. aureus* first by phagocytosis, and then through NETs.** Neutrophils were prestimulated with 10 nM PMA (a) or 100 mU/ml GO (b) for the indicated time or left unstimulated (a and b, 0 min). Before infection with *S. aureus* (MOI 1), the cells were treated with DNase or not (untreated). In the absence of DNase (open bars, untreated), neutrophils kill bacteria by both phagocytosis and NETs. In the presence of DNase, the NETs are dismantled and bacteria are killed only by phagocytosis. The differences in bacterial killing in cultures with and without DNase reflect the antimicrobial activity of NETs. Neutrophils that were not prestimulated killed *S. aureus* efficiently exclusively by phagocytosis because treatment with DNase did not affect the killing. However, cells prestimulated for 60 min showed decreased bacterial killing. Under both conditions, DNase treatment had no effect on killing the bacteria, as NETs had not yet emerged. After 120 min stimulation, when NETs are formed, DNase reduced killing of *S. aureus*. 3–4 h after stimulation, neutrophils killed *S. aureus* as efficiently as unstimulated cells. This killing was completely caused by NETs, as it was affected by the DNase treatment. (c) Unstimulated and PMA-activated (240 min) neutrophils of patients with CGD showed impaired killing of *S. aureus*. Their defective bacterial killing was circumvented when NETs were induced with GO (for 240 min). The experiment was repeated at least five times with neutrophils from independent donors with similar results. The data shown is a representative triplicate experiment and presented as a mean value ± the SD.

Efficient bacterial killing was observed with naive neutrophils (0 min), and the presence of DNase had no effect, indicating that the antimicrobial activity was exclusively through phagocytosis. 60 min after stimulation, when the neutrophils start to undergo morphological changes but the cells have not made NETs yet (Fig. 2 b), phagocytic killing is decreased and little, if any, NET killing is observed because there is no difference between untreated cultures and cultures incubated with DNase. By 120 min, neutrophils start dying and forming NETs, and from this time point on most of the antimicrobial activity in the culture is NET mediated. Infection of neutrophils that were activated for 240 min, where the cells were dead and had formed the maximal amount of NETs, showed that NET killing can be as effective as phagocytosis (compare to time 0). Similar results were obtained if either PMA or GO were used for prestimulating the cells.

As expected, neutrophils from CGD patients, whether PMA stimulated or not, showed impaired killing of *S. aureus* because ROS are required for phagosomal killing and to make NETs (Fig. 7 c). Interestingly, when neutrophils from CGD patients were stimulated with GO for 240 min, bypassing the requirement of NADPH oxidase for NET formation, *S. aureus* was killed very efficiently. This killing activity was mediated by NETs because it was completely abrogated by DNase treatment. These data further support our finding that NADPH oxidase is essential not only for phagosomal killing (Fang, 2004; Segal, 2005) but also for NET formation. The additive roles of this enzyme likely explain the severe clinical infections of patients with CGD.

Discussion

NET formation is a potent antimicrobial mechanism of neutrophils. NETs have been documented in vivo in several pathological conditions, including appendicitis, experimental models of shigellosis (Brinkmann et al., 2004), and preeclampsia (Gupta et al., 2005). Furthermore, the importance of NETs in host defense was recently demonstrated in models for necrotizing fasciitis (Buchanan et al., 2006) and pneumonia (Beiter et al., 2006). The release of intact chromatin into the extracellular space is unprecedented. We describe that after activation, the neutrophils become highly phagocytic and eventually undergo morphological changes that lead to NET formation (Figs. 1 and 2 and Videos 1 and 2, available at http://www.jcb.org/cgi/content/full/jcb.200606027/DC1). The changes follow a particular pattern that is initiated by the loss of nuclear segregation into eu- and heterochromatin. Simultaneously, the characteristic lobular form of the nucleus is also lost. At this point the nuclear membranes (Fig. 2) start to separate from each other, but the morphology of cytoplasm and organelles seem intact. At later time points, the nuclear envelope disintegrates into vesicles (Fig. 3) and the granular membranes disappear, allowing the mixing of nuclear, cytoplasm, and granular components. Throughout this process the cell membrane is intact, and only after the chromatin and granular components are mixed does it break, allowing the extrusion of the NETs.

The mechanism of NET formation is clearly distinct from apoptosis (Fadeel et al., 1998) because there is no DNA fragmentation, PS is not exposed before cell death, and the morphological characteristics of these two forms of active cell death are very different (Fig. 4). Furthermore, caspases, which are proteases that are the executioners of apoptosis, do not seem to be involved in the process of NET formation (unpublished data). There are several reports about apoptosis in activated neutrophils (Fadeel et al., 1998; Lundqvist-Gustafsson and Bengtsson, 1999; Hampton et al., 2002). Apoptosis was shown to depend on the production of ROS, independent from caspases, and does not feature DNA fragmentation. These observations seem inconsistent with the data presented here. The discrepancy is likely caused by several differences in the experimental setup. We performed all our experiments with adherent neutrophils and in the absence or low concentrations of serum, which mimics conditions at inflammatory sites. Many of the published results on induction of ROS-dependent apoptosis were performed with neutrophils in suspension and the presence of high concentrations of serum, which inhibits NET formation (Fig. S2). Furthermore, cells that have lost their membrane integrity were not considered (Lundqvist-Gustafsson and Bengtsson,

1999; Hampton et al., 2002). This might have excluded neutrophils that had potentially made NETs. It would be interesting to reanalyze NET formation under the conditions used by other investigators. In addition, our data are consistent with previous studies showing that the cytotoxicity induced by PMA and hydrogen peroxide (Tsan, 1980; Tsan and Denison, 1980; Takei et al., 1996) in neutrophils is ROS dependent and different from apoptosis because it is caspase independent, does not induce DNA fragmentation, and has unique morphological features, such as the loss of nuclear membrane.

Necrosis is also distinct from the process of NET formation. The most apparent difference is the morphological change of the nucleus preceding the formation of NETs. While in necrosis, the nuclear envelope remains intact (Fig. 4), whereas early in the process that leads to NETs, the nuclear membranes disintegrate into a multitude of vesicles, allowing the mixing of nuclear components and granular material. Another clear difference is the requirement for specific cellular activation and the assembly and activity of the NADPH oxidase in the case of NET formation. The conclusion of our results is that NET formation is the consequence of a novel form of active cell death.

We consistently observe that, depending on the stimuli and donor (Fig. S5, available at http://www.jcb.org/cgi/content/full/jcb.200606027/DC1), only a certain percentage of the neutrophils in a culture make NETs. The significance of this observation is not clear. Experiments with neutrophils seeded at very low numbers show that the majority of neutrophils in circulation are capable of making NETs (unpublished data). This suggests that in neutrophil cultures, and maybe also in vivo, there are mechanisms to regulate which neutrophils start a program that culminates in NET formation.

To investigate the signaling pathway contributing to NET formation, it was important to exclude preactivation of cells during the isolation procedure. Initial observations of NETs were from neutrophils isolated by a dextran/ficoll method (Weinrauch et al., 2002). As was also observed by others (Rebecchi et al., 2000), some neutrophil dextran/ficoll preparations were preactivated, which lead to high background of NETs in unstimulated controls. Interestingly, this isolation method may cause ROS production in neutrophils (Rebecchi et al., 2000). The data presented here was generated with neutrophils isolated by percoll density-gradient centrifugation. This method avoids steps like dextran erythrocyte sedimentation and lysis (Aga et al., 2002), which activate cells. Using this method, we routinely isolated >98% pure and unstimulated neutrophils from human blood. We also observed that IL-8 and LPS induce NETs less efficiently than bacteria. We propose that optimal NET formation requires activation through multiple receptors. Further experiments should address this point.

In our initial description of NETs (Brinkmann et al., 2004), we suggested, based on indirect evidence, that NETs are actively released from living neutrophils. We show, using live-cell imaging (Figs. 1, S3, and S4), the status of individual neutrophils from activation to NET formation, and demonstrate that NET formation is the final step in a program of active cell death and that NETs are released in the moment an activated neutrophil dies.

We show, pharmacologically and genetically, that ROS produced by the NADPH oxidase are required, and that hydrogen peroxide is sufficient for the formation of NETs (Figs. 5 and 6). Indeed, it is interesting that, although PMA has many effects in the cells besides the activation of NADPH oxidase through PKC activation, the morphology of cells treated with PMA and GO share morphological changes like nuclear membrane disintegration, chromatin relaxation, mixing of cytoplasmic and nuclear components, and other features of cell death that result in NETs. Because catalases decompose hydrogen peroxide to water and oxygen, they regulate NET formation. The inhibition of neutrophil catalases resulted in a dramatic increase of NET formation, whereas exogenous catalases had an inhibitory effect. Because catalases are commonly found in bacteria, it is conceivable that microbes use catalases to regulate NET formation (Mandell, 1975).

Our data show that ROS function as signaling molecules (Reth, 2002; Rhee et al., 2005; Torres et al., 2005), but the nature of the downstream signaling is still unclear. It has been shown that the oxidation of the active cysteine in phosphatases (Tonks, 2005) to sulfenic acid transiently inactivates these enzymes. This ROS-dependent modification happens at ROS concentrations that are present in activated neutrophils. The oxidized form of proteins is extremely short lived; therefore, it is difficult to determine the specific targets of ROS in neutrophils. Also, Reeves et al. (2002) suggested that ROS production in neutrophils might function as second messengers that alter the granular physiology. Indeed, they show that ROS induce modifications in the phagocytic vacuole that are reminiscent of the initial changes in the neutrophils before formation of NETs.

The implications of our results are that the severe immunodeficient phenotype of CGD patients might be linked to NET formation (Fig. 6). The lack of NADPH oxidase activity might have different effects, including the reduction in the direct antimicrobial activity of ROS (Hampton et al., 1998), the lack of granule content release (Reeves et al., 2002), and the inability to make NETs. The catastrophic consequences of mutations in NADPH oxidase might be a combination of these three effects.

At this point, it is unclear why only granular, and not cytoplasmic, proteins were observed decorating the NETs (Brinkmann et al., 2004). Our results suggest that the chromatin is also in contact with the cytoplasm (Fig. 2 k), but it is probable that the interaction between granular proteins and chromatin are based on charge because most of the granular proteins observed on NETs are highly cationic and might avidly bind to DNA. Further investigations will have to comprehensively determine the molecular composition of NETs and clarify whether, indeed, there are cytoplasmic proteins present in them.

Neutrophils are terminally differentiated when they leave the bone marrow, and they have a short life span in circulation (Squier et al., 1995). Their fate is either to be cleared from circulation or recruited to an inflammatory site. Upon microbial challenge, neutrophils are activated, and, initially, they become phagocytic. In our in vitro models, during the first 60 min, phagocytosis is the main mechanism to clear microbes (Fig. 7). 120 min after stimulation, their phagocytic capacity is restricted.

At this point, the second antimicrobial mechanism takes over. Nuclear and granular components mingle in the cytoplasm and are rapidly released when the neutrophils finally die, filling up the extracellular space with antimicrobial NETs.

A hitherto unknown form of active cell death apparently evolved to allow neutrophils to kill microbes post mortem. In this form of cell death, the potent cationic antimicrobial peptides and proteins of neutrophils are mixed with chromatin and released to form NETs. Interestingly, the generation of ROS by NADPH oxidase is required for efficient phagocytic killing, and ROS act as a second messenger to trigger NET formation. Importantly, in this form of cell death DNA fragmentation is not activated, allowing the chromatin to unfold in the extracellular space. NETs can bind and kill microbes by providing a high local concentration of antimicrobial peptides and, at the same time, minimize tissue damage by sequestering the noxious granule enzymes. The novel form of active cell death allows neutrophils to pursue their antimicrobial battle even beyond their life span.

Materials and methods

Cells and cell culture

Human neutrophils and PBMCs were isolated from healthy donors or patients with CGD using density gradient separation (Aga et al., 2002). For control experiments, we isolated neutrophils by a dextran/ficoll method (Weinrauch et al., 2002). Patients with CGD were recruited in the Centre for Patients with Primary Immunodeficiency (Charité Medical University, Berlin). Diagnosis of CGD was determined by DHR test and genetic analysis of NADPH components, and was confirmed by chemiluminescence. All patients and controls gave written consent and the study was approved by the ethics committee of the Charité. If not stated otherwise, cells were resuspended in RPMI medium (phenol red–free) supplemented with 10 mM Hepes and 2% human serum albumin. 5×10^5–10^6 neutrophils/ml were seeded into tissue culture plates, glass, collagen-coated glass, collagen-coated glass for live cell imaging, or on glass coverslips for immunofluorescence pretreated with 0.001% polylysine. Incubations were performed at 37°C in the presence of 5% CO_2.

Stimulation and inhibition of NET formation

S. aureus 8324–5 (provided by R. Novick, New York University, New York, NY) was grown to exponential phase in brain heart infusion medium with aeration. Bacteria were washed twice with chilled PBS. 2×10^7 bacteria/ml were added to 10^6 neutrophils/ml in the presence of 0.5% heat-inactivated serum. Bacteria were centrifuged onto the neutrophils at 200 g and 37°C. The following stimuli were used at indicated concentrations: 1 μg/ml LPS in combination with 500 ng/ml of LPS-binding protein (Biometec), IL-8 at 100 ng/ml, PMA at 10–20 nM, and 100 mU/ml of the H_2O_2-producing enzyme GO (Worthington Biochemical Corp.). Neutrophils were incubated with inhibitors 30 min before stimulation. The NADPH oxidase inhibitor DPI (Calbiochem) was used at 5–10 μM and the catalase inhibitor AT (Calbiochem) at 1 mM. Catalase (Worthington Biochemical Corp.) was used at 100 U/ml. Heat-inactivated fetal calf serum was used at concentrations ranging from 5–20% to inhibit NET formation.

Transmission electron microscopy

For fine structural analysis, cells were fixed with 2.5% glutaraldehyde, postfixed with 1% osmiumtetroxide, contrasted with uranylacetate and tannic acid, dehydrated, and embedded in Polybed (Polysciences). After polymerization, specimens were cut at 60 nm and contrasted with lead citrate. For immunodetection, cells were fixed with 4% PFA and embedded in a mixture of 25% sucrose/10% PVA. Ultrathin sections were cut at −105°C, blocked, and reacted with primary antibodies (anti-LBR; Epitomics), followed by secondary antibodies coupled to 6- or 12-nm gold particles. Specimens were analyzed in a Leo 906E transmission electron microscope (Oberkochen) using digital cameras (Ultraview and Morada; SIS).

Immunofluorescence assays

Neutrophils were seeded on glass coverslips treated with 0.001% polylysine, allowed to settle, and treated with PMA (25 nM) or left unstimulated. Cells were fixed with 4% PFA, blocked (3% normal donkey serum, 3% cold water fish gelatin, 1% bovine serum albumin, and 0.05% Tween 20 in PBS) and incubated with primary antibodies antinuclear membrane (ab12365; Abcam); anti–H2A–H2B–DNA complex (Losman et al., 1992); anti-neutrophil elastase (in-house); anti–*S. aureus* (Biodesign), which were detected with secondary antibodies coupled to Cy2 or Cy3 (Dianova). Controls were done with isotype-matched controls. For DNA detection, DRAQ5 (shown) Bisbenzimide 33342 (Hoechst 33342), Sytox, and ToPro3 were used. Specimens were mounted in Mowiol and analyzed with a PlanApo 63×/1.32 NA objective on a confocal microscope (TCS-SP; Leica).

Live cell imaging

2–5 × 10^5 neutrophils were stained with calcein blue AM (Invitrogen) and seeded into culture dishes equipped with glass bottoms (Mattek). The medium contained Annexin V (1:50; Invitrogen, labeled with Alexa Fluor 488; or Abcam, labeled with Cy3) and Fabs against the H2A–H2B–DNA complex (Losman et al., 1992) directly coupled to Atto 555 or against neutrophil elastase (in house) directly coupled to Atto 488 at a concentration of 2 μg/ml. Cells were stimulated with 20 nM PMA and recorded at 37°C on a microscope (Axiovert 200M; Carl Zeiss MicroImaging, Inc.) with a Plan-Neofluar 100×/1.3 NA objective over a period of 4 h. Each minute, a set of four images (phase contrast, blue, green, and red fluorescence) was taken with a camera (Orca ER; Hamamatsu). The system was controlled by the Openlab software (Improvision). Individual frame overlays and videos were prepared using Volocity software (Improvision).

Isolation and quantification of NETs

NETs generated by activated neutrophils were digested with 500 mU/ml micrococcal nuclease (MNase; Worthington Biochemical Corp.). The nuclease activity was stopped with 5 mM EDTA and the culture supernatants were collected and stored at 4°C until further use. Total DNA was isolated from naive neutrophils with DNazol supplemented with 1% polyacryl carrier (Molecular Research Center) according to the manufacturer's instructions and solubilized in TE buffer. NETs or genomic DNA was quantified using Picogreen dsDNA kit (Invitrogen) according to manufacturer's instructions. Total DNA of neutrophils and PBMCs was isolated from four different donors and quantified. 10^6 neutrophils had 6.2 μg DNA (±0.27 SD) and 10^6 PBMCs contained 6.3 μg DNA (±0.81 SD). Percentage of released NET-DNA was calculated by dividing the amount of isolated NET-DNA through the average genomic DNA content.

Isolation and quantification of neutrophil elastase

Neutrophils were activated for indicated times with PMA. Neutrophil elastase in suspension was collected in culture supernatants. NET-associated neutrophil elastase and NET-DNA was isolated by incubating the cells in medium containing 500 mU/ml MNase for 10 min. Samples were resuspended in 1 M NaCl 0.02% Triton X-100. Total neutrophil elastase was measured from unstimulated neutrophils lysed with 0.02% Triton X-100 in 1 M NaCl. Neutrophil elastase activity was quantified with 100 μM of the peptide substrate N-(Methoxysuccinyl)-Ala-Ala-Pro-Val 4-nitroanilide for 15 min at room temperature. Optical density was measured at 405 nm (Microplate reader EL800; BIO-TEK Instruments).

Induction of neutrophil apoptosis and necrosis

Neutrophils were incubated with 20 ng/ml anti-Fas (Millipore) antibodies for up to 18 h to induce apoptosis. We induced neutrophil necrosis with secreted toxins from *S. aureus*. Strain 8325–4 was grown overnight in BHI medium. Bacteria were pelleted, supernatants were collected, and the filter was sterilized. Protein concentration was determined using RC DC Protein Assay (Bio-Rad Laboratories). Necrosis was elicited by treating neutrophils with 1 mg/ml of secreted proteins for 15 min.

Quantification and characterization of cell death

Cells were stained by the addition of 2 μM Sytox Green (Invitrogen) and were analyzed by fluorescence microscopy. Apoptosis was detected by TUNEL staining (Promega) according to manufacturer's instructions. At least 250 cells per sample were analyzed.

Determination of ROS production

ROS production was measured by chemiluminescence (Liu et al., 1996). Neutrophils were activated in the presence of 50 μM luminol and 1.2 U/ml

horseradish peroxidase (Calbiochem) and chemiluminescence was detected using a Monolight 3096 (BD Biosciences).

Phagocytic and NET killing of *S. aureus* by neutrophils

S. aureus was grown to exponential phase in brain heart infusion medium with aeration and washed twice with chilled PBS. 10^6 human neutrophils/ml were stimulated for the indicated time points up to 240 min with PMA or GO or left unstimulated. The cells were stimulated at different time points, so all wells were incubated for 240 min, but stimulated for the indicated periods. The cells were further incubated in fresh medium without PMA or GO containing 2% heat-inactivated pooled human serum with or without 100 U/ml DNaseI. The culture was infected with 10^6 *S. aureus* and centrifuged for 10 min at 800 *g* and further incubated for 20 min. After adding 5 mM EDTA, the samples were vortexed for 5 min and the cell suspensions were diluted in chilled PBS with 0.1% Triton X-100. The microbicidal effect observed was the same if the cells were lysed with 0.1% Triton X-100, 0.1% Saponin, or distilled water. Aliquots were plated to determine CFUs. Absence of bacterial killing was defined as the number of bacteria recovered after infection of DNaseI-treated neutrophils that were stimulated for 240 min with PMA or GO. At this time point, all the cells were dead and unable to phagocytose (Fig. 1), and degradation of NETs prevented extracellular killing.

Online supplemental material

Fig. S1 shows the method for quantification of NETs. Fig. S2 shows that serum inhibits NET formation. Video 1 (key frames are depicted in Fig. 1) shows that NETs detected by a chromatin marker are released when the cell membrane ruptures. Fig. S3 and Video 2 show NET formation by using a granular marker. Fig. S4 and Video 3 show that neutrophils isolated from CGD patients make NETs in response to GO. Fig. S5 shows variation in NET formation between neutrophils from different donors. Online supplemental material is available at http://www.jcb.org/cgi/content/full/jcb.200606027/DC1.

The authors would like to thank Britta Laube, Beatrix Fauler, and Annette Wahlbrink for technical assistance, Marc Monastier for the gift of the monoclonal antibody against the histone–DNA complex, and Abdul Hakkim, Bärbel Raupach, Constance Scharff, and Constantin Urban for critical reading of the manuscript.

Y. Weinrauch is supported by the National Institutes of Health.

Submitted: 6 June 2006
Accepted: 5 November 2006

References

Aga, E., D.M. Katschinski, G. van Zandbergen, H. Laufs, B. Hansen, K. Muller, W. Solbach, and T. Laskay. 2002. Inhibition of the spontaneous apoptosis of neutrophil granulocytes by the intracellular parasite *Leishmania major*. *J. Immunol.* 169:898–905.

Beiter, K., F. Wartha, B. Albiger, S. Normark, A. Zychlinsky, and B. Henriques-Normark. 2006. An endonuclease allows *Streptococcus pneumoniae* to escape from neutrophil extracellular traps. *Curr. Biol.* 16:401–407.

Borregaard, N., and J.B. Cowland. 1997. Granules of the human neutrophilic polymorphonuclear leukocyte. *Blood*. 89:3503–3521.

Brinkmann, V., U. Reichard, C. Goosmann, B. Fauler, Y. Uhlemann, D.S. Weiss, Y. Weinrauch, and A. Zychlinsky. 2004. Neutrophil extracellular traps kill bacteria. *Science*. 303:1532–1535.

Buchanan, J.T., A.J. Simpson, R.K. Aziz, G.Y. Liu, S.A. Kristian, M. Kotb, J. Feramisco, and V. Nizet. 2006. DNase expression allows the pathogen group A *Streptococcus* to escape killing in neutrophil extracellular traps. *Curr. Biol.* 16:396–400.

Fadeel, B., A. Ahlin, J.I. Henter, S. Orrenius, and M.B. Hampton. 1998. Involvement of caspases in neutrophil apoptosis: regulation by reactive oxygen species. *Blood*. 92:4808–4818.

Fang, F.C. 2004. Antimicrobial reactive oxygen and nitrogen species: concepts and controversies. *Nat. Rev. Microbiol.* 2:820–832.

Genestier, A.L., M.C. Michallet, G. Prevost, G. Bellot, L. Chalabreysse, S. Peyrol, F. Thivolet, J. Etienne, G. Lina, F.M. Vallette, et al. 2005. *Staphylococcus aureus* Panton-Valentine leukocidin directly targets mitochondria and induces Bax-independent apoptosis of human neutrophils. *J. Clin. Invest.* 115:3117–3127.

Gupta, A.K., P. Hasler, W. Holzgreve, S. Gebhardt, and S. Hahn. 2005. Induction of neutrophil extracellular DNA lattices by placental microparticles and IL-8 and their presence in preeclampsia. *Hum. Immunol.* 66:1146–1154.

Hampton, M.B., A.J. Kettle, and C.C. Winterbourn. 1998. Inside the neutrophil phagosome: oxidants, myeloperoxidase, and bacterial killing. *Blood*. 92:3007–3017.

Hampton, M.B., M.C. Vissers, J.I. Keenan, and C.C. Winterbourn. 2002. Oxidant-mediated phosphatidylserine exposure and macrophage uptake of activated neutrophils: possible impairment in chronic granulomatous disease. *J. Leukoc. Biol.* 71:775–781.

Heyworth, P.G., A.R. Cross, and J.T. Curnutte. 2003. Chronic granulomatous disease. *Curr. Opin. Immunol.* 15:578–584.

Kanthack A, W.B. Hardy 1895. The morphology and distribution of the wandering cells of mammalia. *J Physiol*. 17:80.1–119.

Klebanoff, S.J. 1999. Oxygen metabolites from phagocytes. *In* J.I. Gallin and R. Snyderman, editors. Inflammation: Basic Principles and Clinical Correlates. Lippincott Williams & Wilkins, Philadelphia. 721–768 pp.

Liu, L., C. Dahlgren, H. Elwing, and H. Lundqvist. 1996. A simple chemiluminescence assay for the determination of reactive oxygen species produced by human neutrophils. *J. Immunol. Methods*. 192:173–178.

Losman, M.J., T.M. Fasy, K.E. Novick, and M. Monestier. 1992. Monoclonal autoantibodies to subnucleosomes from a MRL/Mp(-)+/+ mouse. Oligoclonality of the antibody response and recognition of a determinant composed of histones H2A, H2B, and DNA. *J. Immunol.* 148:1561–1569.

Lundqvist-Gustafsson, H., and T. Bengtsson. 1999. Activation of the granule pool of the NADPH oxidase accelerates apoptosis in human neutrophils. *J. Leukoc. Biol.* 65:196–204.

Mandell, G.L. 1975. Catalase, superoxide dismutase, and virulence of *Staphylococcus aureus*. In vitro and in vivo studies with emphasis on staphylococcal–leukocyte interaction. *J. Clin. Invest.* 55:561–566.

Molloy, S. 2006. Bacterial pathogenesis: escaping the net. *Nat. Rev. Microbiol.* 4:242–243.

Nathan, C. 2006. Neutrophils and immunity: challenges and opportunities. *Nat. Rev. Immunol.* 6:173–182.

Rebecchi, I., N. Ferreira Novo, Y. Juliano, and A. Campa. 2000. Oxidative metabolism and release of myeloperoxidase from polymorphonuclear leukocytes obtained from blood sedimentation in a ficoll-hypaque gradient. *Cell Biochem. Funct.* 18:127–132.

Reeves, E.P., H. Lu, H.L. Jacobs, C.G. Messina, S. Bolsover, G. Gabella, E.O. Potma, A. Warley, J. Roes, and A.W. Segal. 2002. Killing activity of neutrophils is mediated through activation of proteases by K+ flux. *Nature*. 416:291–297.

Reth, M. 2002. Hydrogen peroxide as second messenger in lymphocyte activation. *Nat. Immunol.* 3:1129–1134.

Rhee, S.G., S.W. Kang, W. Jeong, T.S. Chang, K.S. Yang, and H.A. Woo. 2005. Intracellular messenger function of hydrogen peroxide and its regulation by peroxiredoxins. *Curr. Opin. Cell Biol.* 17:183–189.

Segal, A.W. 2005. How neutrophils kill microbes. *Annu. Rev. Immunol.* 23:197–223.

Squier, M.K., A.J. Sehnert, and J.J. Cohen. 1995. Apoptosis in leukocytes. *J. Leukoc. Biol.* 57:2–10.

Takei, H., A. Araki, H. Watanabe, A. Ichinose, and F. Sendo. 1996. Rapid killing of human neutrophils by the potent activator phorbol 12-myristate 13-acetate (PMA) accompanied by changes different from typical apoptosis or necrosis. *J. Leukoc. Biol.* 59:229–240.

Tonks, N.K. 2005. Redox redux: revisiting PTPs and the control of cell signaling. *Cell*. 121:667–670.

Torres, M.A., J.D. Jones, and J.L. Dangl. 2005. Pathogen-induced, NADPH oxidase-derived reactive oxygen intermediates suppress spread of cell death in *Arabidopsis thaliana*. *Nat. Genet.* 37:1130–1134.

Tsan, M.F. 1980. Phorbol myristate acetate induced neutrophil autotoxicity. *J. Cell. Physiol.* 105:327–334.

Tsan, M.F., and R.C. Denison. 1980. Phorbol myristate acetate-induced neutrophil autotoxicity. A comparison with H2O2 toxicity. *Inflammation*. 4:371–380.

Urban, C.F., U. Reichard, V. Brinkmann, and A. Zychlinsky. 2006. Neutrophil extracellular traps capture and kill *Candida albicans* yeast and hyphal forms. *Cell. Microbiol.* 8:668–676.

Weinrauch, Y., D. Drujan, S.D. Shapiro, J. Weiss, and A. Zychlinsky. 2002. Neutrophil elastase targets virulence factors of enterobacteria. *Nature*. 417:91–94.

Worman, H.J., J. Yuan, G. Blobel, and S.D. Georgatos. 1988. A lamin B receptor in the nuclear envelope. *Proc. Natl. Acad. Sci. USA*. 85:8531–8534.

Yu, B.P. 1994. Cellular defenses against damage from reactive oxygen species. *Physiol. Rev.* 74:139–162.